Avalanches and scaling collapse in the large-N Kuramoto model

J. Patrick Coleman,* Karin A. Dahmen, and Richard L. Weaver
Department of Physics, University of Illinois, 1110 West Green Street, Urbana, Illinois 61801, USA

(Received 22 December 2017; published 27 April 2018)

We study avalanches in the Kuramoto model, defined as excursions of the order parameter due to ephemeral episodes of synchronization. We present scaling collapses of the avalanche sizes, durations, heights, and temporal profiles, extracting scaling exponents, exponent relations, and scaling functions that are shown to be consistent with the scaling behavior of the power spectrum, a quantity independent of our particular definition of an avalanche. A comprehensive scaling picture of the noise in the subcritical finite-N Kuramoto model is developed, linking this undriven system to a larger class of driven avalanching systems.

DOI: 10.1103/PhysRevE.97.042219

I. INTRODUCTION

Scale free dynamics have been shown to be characteristic of systems exhibiting phase transitions [1]. Progress has been made lately in understanding fluctuations in systems that are undergoing phase transitions. Many systems far from thermal equilibrium exhibit avalanches across many orders of magnitude in size. The statistics of these avalanches are often found to be in accord with simple models [2]. The scaling behavior of the avalanche statistics and dynamics is independent of the microscopic details (i.e., universal) and shared among disparate systems including slip motion in metallic glasses [3,4], Barkhausen noise in magnets [5,6], earthquakes [7], and stellar light curves [8].

While much work has been done on avalanches near depinning transitions of elastic interfaces, such as magnetic domain walls, elastic charge density waves, and other systems [2], few avalanche studies have been done on plastic systems with many interacting domain walls, such as the random field Ising model [2] and plastic charge density wave depinning systems [9]. The system we study here shares many traits with these plastic avalanche systems, though differing notably in lacking an external driving force.

Synchronizing coupled phase oscillators, of which the $N \to \infty$ Kuramoto model is a prototype, exhibit a phase transition, passing from an incoherent state at weak coupling to a synchronized state at strong coupling. The Kuramoto model is of particular interest because it admits analytic solutions [10,11]. The model has numerous generalizations that are studied numerically and analytically.

Finite-size effects near criticality have been explored [12–15]. Choi *et al.* studied the effect of system size on the evolution of the order parameter from total coherence or incoherence toward its steady-state value at criticality [12]. Daido, Hong, and others studied fluctutations in the order parameter's steady-state behavior as a function of system size near criticality [13–15].

Synchronizing coupled oscillators, like those of the Kuramoto model, have been recognized as elements in classical analogs for lasers [16–19]. We anticipate that studies of their subcritical statistics could be relevant to the onset of lasing.

Critical systems such as the Kuramoto model have also been studied as promising models of brain dynamics [20].

Here we carry out numerical simulations of finite-N Kuramoto systems below criticality and examine the time-dependent fluctuations as groups of oscillators spontaneously synchronize and fall out of synchronization. We offer evidence of avalanches in the Kuramoto model whose statistics and dynamics show scaling behavior in a broad region below the critical coupling strength. We report avalanche statistics in the Kuramoto model and find that the scaling forms applicable to these undriven avalanches are analogous to those of avalanches in externally driven systems [2]. New scaling exponents and scaling functions associated with the underlying nonequilibrium phase transition are extracted. We find that the distributions of these avalanches at different coupling strengths collapse into a single universal curve.

II. MODEL

The Kuramoto model consists of a collection of interacting phase oscillators, each governed by a simple first order differential equation:

$$\frac{d\theta_j}{dt} = \omega_j + \frac{K}{N}\sum_{k=1}^{N}\sin(\theta_k - \theta_j), \tag{1}$$

where θ_j is the phase of the jth oscillator at time t, ω_j is its natural speed, N is the number of oscillators, and K is the coupling strength. The unit of time for these simulations is arbitrary, but for simplicity we will refer to our units of time as seconds, and so the ω_j are in radians per second. These governing equations can be simplified by defining an order parameter

$$r\,e^{i\phi} \equiv \frac{1}{N}\sum_{j=1}^{N} e^{i\theta_j}, \tag{2}$$

*jpcolem2@illinois.edu

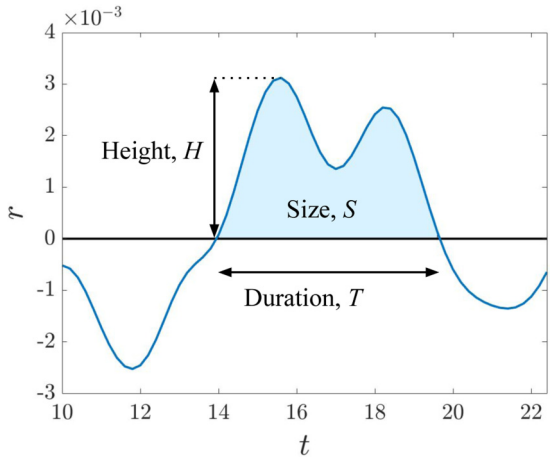

FIG. 1. Definition of avalanche metrics. An avalanche is defined as the section of the order parameter between two consecutive zero crossings. The height H of an avalanche is the maximum height of the order parameter, the size S is the area under the $r(t)$ curve, and the duration T is the time between the two zero crossings.

where ϕ is real and r is real and bounded between zero and one, one corresponding to a state in which all phases are equal.

The governing equations can be rewritten as

$$\frac{d\theta_j}{dt} = \omega_j + Kr\,\sin(\phi - \theta_j), \tag{3}$$

making it clear that the oscillators are coupled to the mean field. Often the ω_j are chosen from a unimodal distribution centered on zero, such as a Gaussian or a Lorentzian distribution.

The Kuramoto model as described thus far has been studied extensively. Here we alter this model so as to make the system more analogous to another system that exhibits phase transitions and avalanches, spontaneous magnetization in the random field Ising model of ferromagnetism [2,5,21].

We modify the Kuramoto model by including, for every oscillator, a second, "mirroring" oscillator which has the same natural speed, but with the opposite sign. The position of the mirror oscillator is always $2\pi - \theta_j$ where θ_j is the position of the oscillator being mirrored. Thus, if we imagine that the oscillators are traveling on the unit circle in the complex plane, the distribution of oscillators is always symmetric about the real axis. The order parameter is therefore always real, and Eq. (2) can be written

$$r = \frac{2}{N}\sum_{j=1}^{N/2}\cos(\theta_j), \tag{4}$$

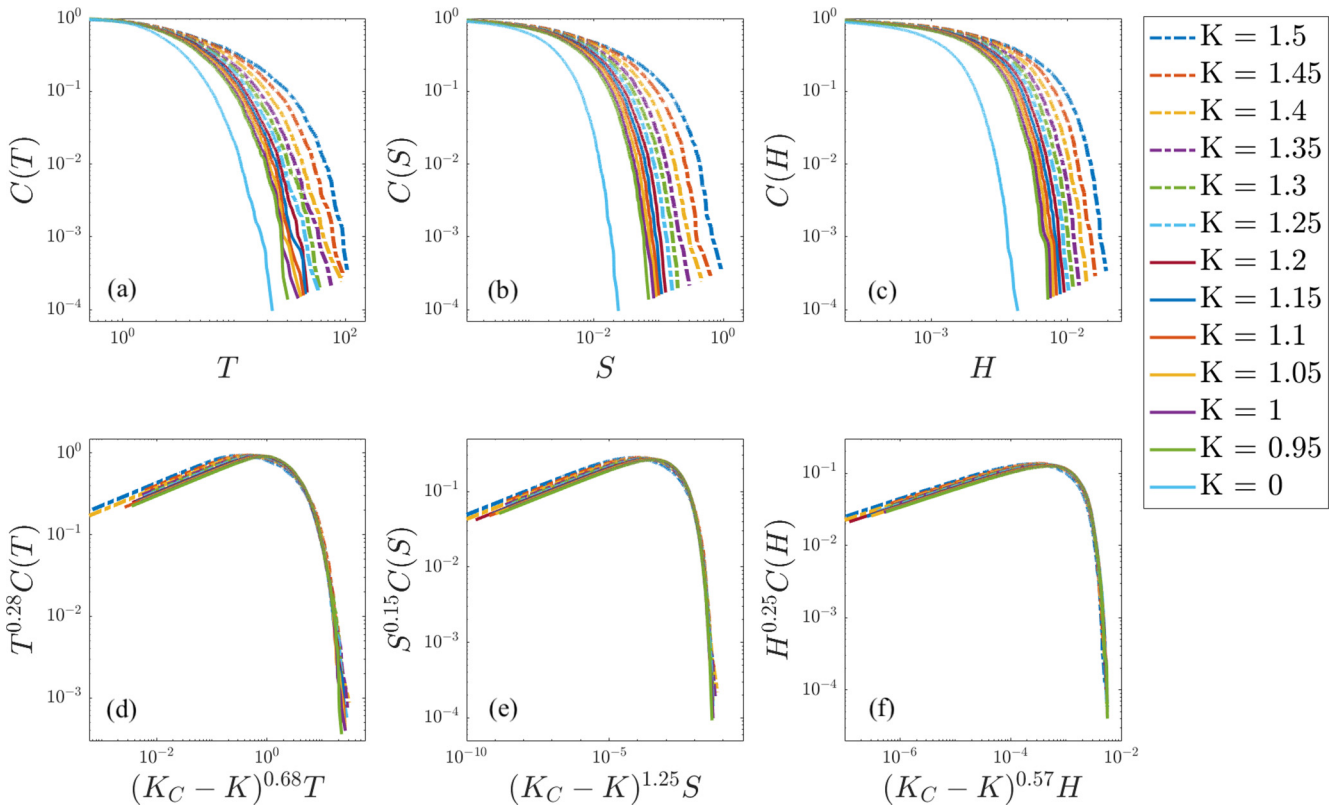

FIG. 2. (a)–(c) Complementary cumulative distribution functions (CCDF) of the avalanche durations, T, sizes, S, and heights, H, for 13 values of the coupling strength K. (d)–(f) Corresponding collapse of the CCDFs by rescaling the x and y axes. The CCDF corresponding to $K = 0$ is not included in the collapses because it is not expected to collapse. The number of avalanches observed for each value of K was between 2945 and 10 377. The critical coupling value is $K_C \approx 1.596$. The tails on the left side of the CCDFs correspond to the smallest avalanches, which are distorted due to their durations being comparable to the time step. As such, the long left tails of the CCDFs ought not be expected to collapse.

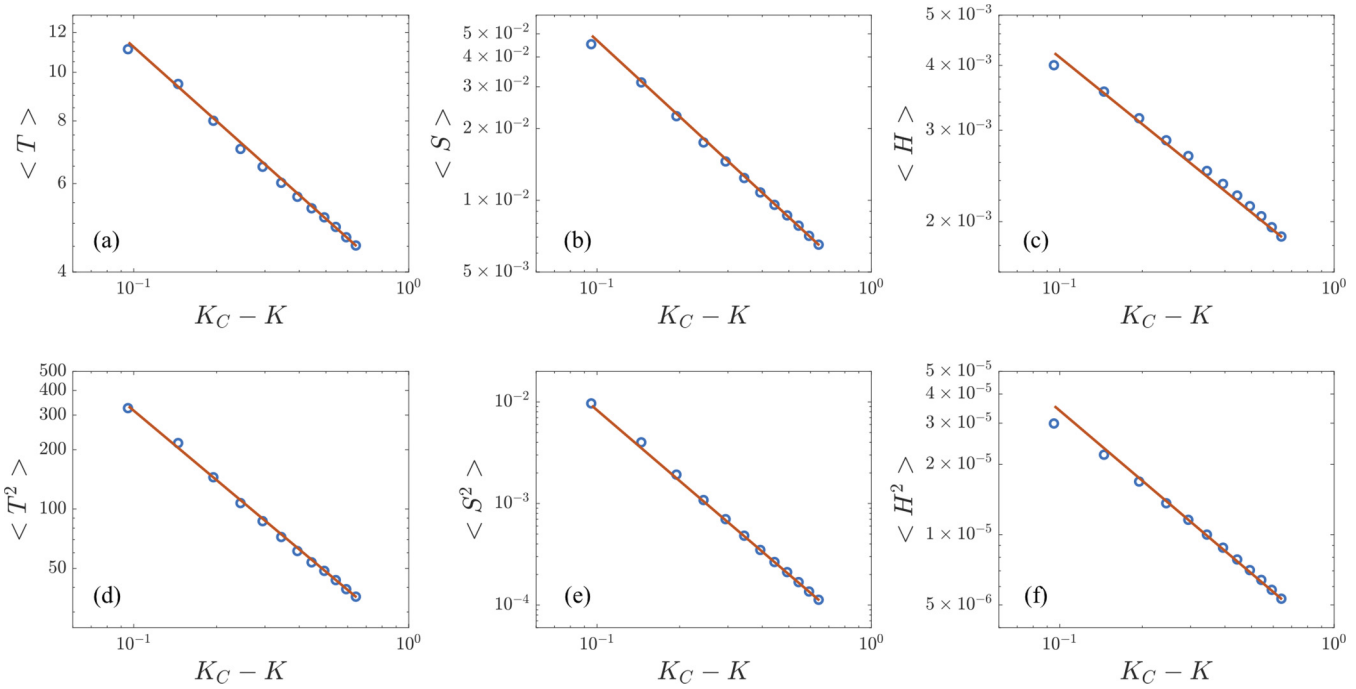

FIG. 3. (a)–(c) Average duration, T, size, S, and height, H, of avalanches for each value of the coupling constant K are shown, where $K_C = 1.596$. The constant slope on the log-log plot reveals that there is a power-law relationship between the average values and distance from criticality. The slopes for (a)–(c) are $-\nu z(-\alpha+2) = -0.49$, $-1/\sigma(-\tau+2) = -1.06$, and $-\rho(-\mu+2) = -0.43$, respectively. (d)–(f) The average square duration, size, and height of the avalanches are shown to be related to $K_C - K$ by a power law. The slopes for (d)–(f) are $-\nu z(-\alpha+3) = -1.2$, $-1/\sigma(-\tau+3) = -2.3$, and $-\rho(-\mu+3) = -1.0$, respectively. The power-law relationships, as well as the values of the scaling exponents, are given in Table I.

such that the order parameter takes values $-1 \leqslant r \leqslant 1$, and the phase angle ϕ is no longer necessary. Equation (3) is unchanged, though now $\phi = 0$ due to the new symmetry. This modification permits us to define avalanches without the introduction of an arbitrary threshold.

For $N \to \infty$ and a unimodal distribution of natural frequencies $g(\omega)$ centered on zero, the Kuramoto equations have a simple solution with a phase transition [11]. A critical coupling strength K_C can be defined that depends on $g(\omega)$. For values of the coupling strength $K < K_C$, the order parameter is zero and the oscillator phases are evenly distributed between zero and 2π. At $K = K_C$, a continuous phase transition occurs and the order parameter scales as $r \propto (K - K_C)^{1/2}$ for $K > K_C$ with $K_C = 2/(\pi g(0))$ [11].

For finite N, the Kuramoto model behaves similarly [10]. We find that for K sufficiently less than K_C, the order parameter fluctuates around zero. As K approaches K_C from below these fluctuations grow, and for K sufficiently greater than K_C the order parameter spontaneously synchronizes. Our model with the mirror oscillators behaves in the same way, but when the

TABLE I. Scaling forms and scaling exponents. The values of the six scaling exponents are listed in the first three rows of the right column. The scaling forms follow those used in Refs. [8,22]. The scaling functions of the CCDFs, F_T, F_S, and F_H, as well as that of the power spectrum, F_P, are not known analytically. However, the scaling functions for the avalanche shapes, G_S and G_T, are known and given in the right column. The scaling relation at the bottom connects the scaling exponents from the three different metrics.

Avalanche duration CCDF	$C(T) \sim T^{-\alpha+1} F_T(T(K_C - K)^{\nu z})$	$\alpha = 1.28 \pm 0.05$, $\nu z = 0.68 \pm 0.05$
Avalanche size CCDF	$C(S) \sim S^{-\tau+1} F_S(S(K_C - K)^{1/\sigma})$	$\tau = 1.15 \pm 0.1$, $1/\sigma = 1.25 \pm 0.1$
Avalanche height CCDF	$C(H) \sim H^{-\mu+1} F_H(H(K_C - K)^{\rho})$	$\mu = 1.25 \pm 0.1$, $\rho = 0.57 \pm 0.1$
Average duration	$\langle T \rangle \sim (K_C - K)^{-\nu z(-\alpha+2)}$	$-\nu z(-\alpha+2) = -0.49$, $K_C = 1.596$
Average size	$\langle S \rangle \sim (K_C - K)^{-1/\sigma(-\tau+2)}$	$-1/\sigma(-\tau+2) = -1.06$
Average height	$\langle H \rangle \sim (K_C - K)^{-\rho(-\mu+2)}$	$-\rho(-\mu+2) = -0.43$
Average square duration	$\langle T^2 \rangle \sim (K_C - K)^{-\nu z(-\alpha+3)}$	$-\nu z(-\alpha+3) = -1.2$
Average square size	$\langle S^2 \rangle \sim (K_C - K)^{-1/\sigma(-\tau+3)}$	$-1/\sigma(-\tau+3) = -2.3$
Average square height	$\langle H^2 \rangle \sim (K_C - K)^{-\rho(-\mu+3)}$	$-\rho(-\mu+3) = -1.0$
Avalanche shape for constant duration	$\langle r \vert T \rangle \sim T^{1-1/\sigma\nu z} G_T(t/T)$	$G_T(x) = Ax(1-x)$; $\sigma\nu z = 0.54$
Avalanche shape for constant size	$\langle r \vert S \rangle \sim S^{1-\sigma\nu z} G_S(t/S^{\sigma\nu z})$	$G_S(x) = Bx\ \exp(-Cx^2/2)$
Power spectrum	$P(\omega) \sim \omega^{-1/\sigma\nu z} F_P(\omega(K_C - K)^{-\nu z})$	$-1/\sigma\nu z = -1.8$, $\nu z = 0.68$
Scaling relation	$(\tau-1)1/\sigma = (\alpha-1)\nu z = (\mu-1)\rho$	

order parameter synchronizes it must choose either a positive or a negative value. This behavior is analogous to spontaneous magnetization in Ising ferromagnets, where the magnetization fluctuates around zero for temperatures above the critical temperature and spontaneously chooses either positive or negative magnetization for temperatures below the critical temperature. Our interest, motivated by studies of avalanches in other finite systems near a phase transition [3,4], is in the fluctuations of r away from zero and how those fluctuations scale near the transition.

We ran simulations for $N = 10^6$ oscillators. Thirteen coupling strengths were simulated: $K = 0.95, 1.00, 1.05, \ldots, 1.50$ and $K = 0$. The natural speeds of the oscillators, ω_j, were drawn randomly from a Gaussian distribution centered on zero with unit variance, and hence the critical coupling strength as $N \to \infty$ is $K_C = 2\sqrt{\frac{2}{\pi}} \approx 1.596$ [11]. For each value of K, twenty simulations were run, each with different natural speeds ω_j and different initial positions for the oscillators. The initial positions were randomly chosen in the range $(0–2\pi)$. The system of equations in Eq. (3) was solved numerically using the Runge-Kutta four method. Each simulation ran for 2^{13} time steps with a step size of 0.2 s. We analyze the entire time trace of the order parameter, $r(t)$. As shown by Choi *et al.* [12], the Kuramoto model shows transient behavior when its initial condition is different from its steady state. But the duration of the transient behaviors seen by Choi *et al.* were short enough, given our system size and distance from criticality, that they should not have an effect on our results here. As a further check that the initial conditions were not distorting the avalanche statistics, 36 simulations were done for $K = 1.15$ with 2^{15} time steps, and complementary cumulative distribution functions (CCDFs) from the first 2^{13} time steps were compared to those from the last 2^{13} time steps. No noticeable differences between these CCDFs were observed.

We analyze the order parameter as a function of time. As the order parameter oscillates around zero, an avalanche is defined as the section of the order parameter between two consecutive zero crossings. We analyze the statistics of the avalanche heights, sizes, and durations as defined in Fig. 1. The avalanche height is the maximum value of $r(t)$ over the time interval between two zero crossings, the size is the area under the $r(t)$ curve between the two zero crossings, and the duration is the length of time between the zero crossings. Due to symmetry in r, which has $\langle r \rangle = 0$ for $K < K_C$, we analyze avalanches for negative values of $r(t)$ as well as positive values, treating their heights and sizes as positive values.

III. ANALYSIS

We show CCDFs of the avalanche heights, sizes, and durations in Fig. 2. As the coupling constant K approaches K_C from below, we observe increases in the magnitudes of all three of these metrics. For the same total simulated time for each value of K, the number of avalanches observed is greater for weak coupling, as we would expect due to the increasing duration of avalanches for stronger coupling. For $K = 0$ the total number of avalanches observed was 10 377, and for $K = 1.5$, the largest value of K we considered, the

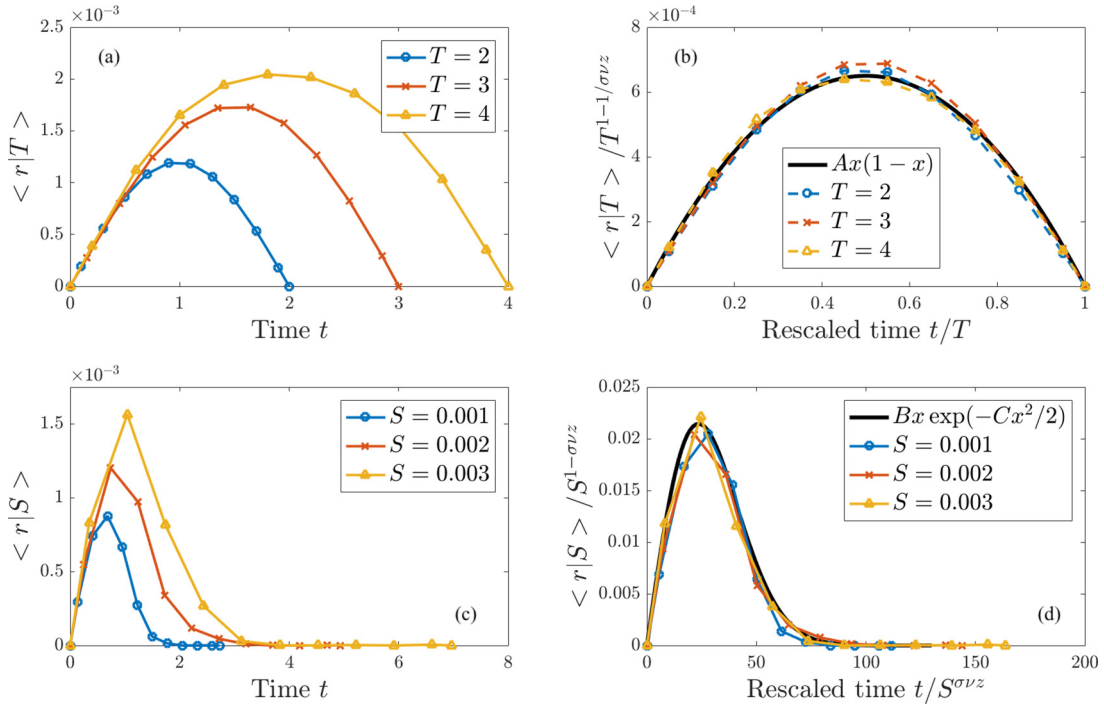

FIG. 4. (a),(b) Average order parameter value as a function of time for avalanches of a certain duration, T, and the corresponding collapse. The average was for all avalanches with duration T to $T + T/10$. These curves are collapsed onto a scaling function of $Ax(1-x)$ where $x = t/T$ by rescaling the y axis by a factor of $T^{1-1/\sigma\nu z}$ as shown. (c),(d) The average order parameter value for avalanches of a certain size, S, and the corresponding collapse. The average was for all avalanches with size S to $S + S/10$. The curves are collapsed after rescaling the y axis by $S^{1-\sigma\nu z}$ and the x axis by $S^{\sigma\nu z}$. The curve on which the lines collapse in (d) is $Bx\ \exp(-Cx^2/2)$, where $x = t/S^{\sigma\nu z}$. For these plots $\sigma\nu z = 0.54$ as given in Table I. The avalanches were extracted from simulations with coupling strength $K = 1.35$.

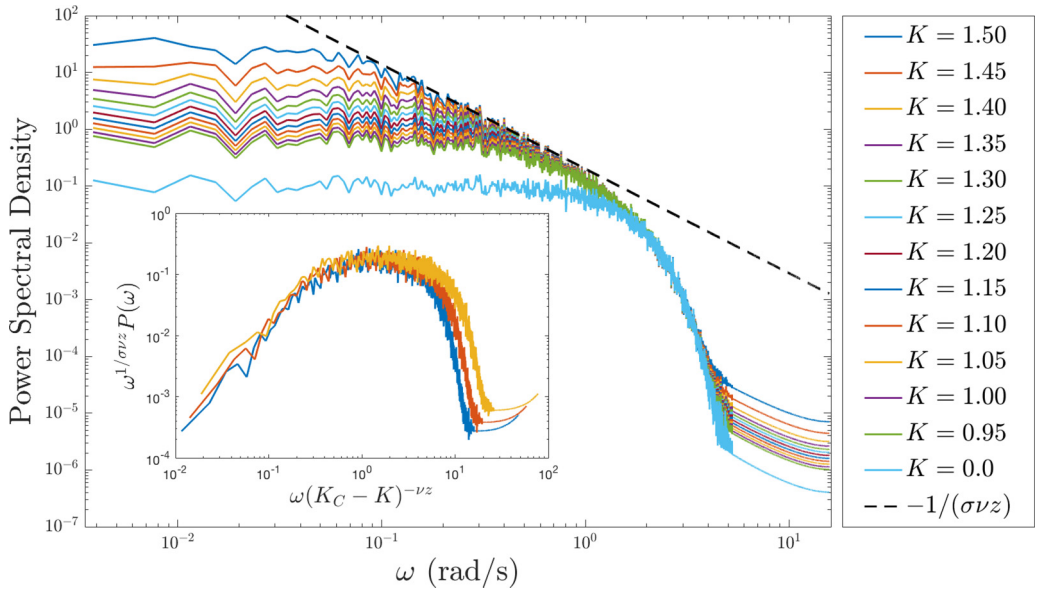

FIG. 5. Power spectral density of the order parameter for each value of coupling constant K. The power-law scaling regime grows as K approaches criticality. The slope of the power law in the scaling regime is $-1/\sigma\nu z = -1.8$ in accord with the values given in Table I. The roll off at high frequencies appears universal, but is presumably related to the Gaussian distribution of natural oscillator speeds. The inset shows a collapse of the three highest K values using the scaling form from Table I. The values of the scaling exponents are consistent with those used in the collapse of the avalanches, $1/\sigma\nu z = 1.8$ and $\nu z = 0.68$. As expected, the collapse works well at low frequencies, where the tested scaling form is predicted to apply.

number of avalanches observed was 2945. All other values of K had a total number of avalanches between these two limits.

We find that by rescaling the axes of the CCDFs, we are able to make the curves collapse, revealing the universal scaling functions shown in Fig. 2. The x axes were rescaled by a factor of $(K_C - K)$ raised to a universal scaling exponent, νz, $1/\sigma$, and ρ for durations, sizes, and heights, respectively. The y axes were rescaled by a factor of the metric raised to another universal scaling exponent, $(1 - \alpha)$, $(1 - \tau)$, and $(1 - \mu)$ for durations, sizes, and heights, respectively. The scaling exponents describe the effect of the coupling strength on the excursions of the order parameter. The scaling forms, along with the values of the scaling exponents, are given in Table I following the conventions used in Ref. [22]. The scaling exponents extracted from these collapses are consistent with the relation $(\tau - 1)1/\sigma = (\alpha - 1)\nu z = (\mu - 1)\rho$, which results from the fact that the number of avalanches in the scaling regime is the same, whether they're counted using the duration, size, or height CCDF.

We calculated the average duration, size, and height of the avalanches for each value of the coupling strength. We also calculated the average square value of each metric as well. The results are shown in Fig. 3. The average values of these metrics are related to the distance from criticality by a power law. Table I shows the scaling laws and the values of the scaling exponents. The scaling forms shown in Table I are derivable from the assumption that the probability distribution function of a given metric (duration T, size S, or height H) scales like a power law with a quickly decaying cutoff function: $P(X) \sim X^{-p_X} f_X(X(K_C - K)^{q_X})$, where X is either T, S, or H, p_X is α, τ, or μ, respectively, q_X is νz, $1/\sigma$, or ρ, respectively, and f_X is a corresponding scaling function with a quickly decaying cutoff at large values of its argument.

We extract the average avalanche shapes for avalanches of three different durations, taken from $K = 1.35$ in Fig. 4. To extract the average avalanche shape for avalanches of a given duration, we take the value of the order parameter at certain points in rescaled time, and average those values. This is done for all avalanches whose duration falls within 10% of the duration being considered. We find that by rescaling the y axis by $T^{1-1/\sigma\nu z}$, we can collapse the three plots on to a curve $Ax(1 - x)$, where $A = 2.6 \times 10^{-3}$ and $x = t/T$.

We show the average avalanche profile for avalanches of a given size as well in Fig. 4. By rescaling the x axis by $S^{\sigma\nu z}$ and the y axis by $S^{1-\sigma\nu z}$, we collapse the profiles for three different sizes, again for $K = 1.35$. The plots of the average avalanche profiles for fixed size were made by sampling all avalanches within 10% of the given size at certain times and averaging the value of the order parameter at those points. The long tails are due to the fact that the start of an avalanche is defined to be at $t = 0$, but the avalanches have various durations, so at times after an avalanche has ended, its order parameter value is $r = 0$. So, for example, at $t/S^{\sigma\nu z} = 80$, $\langle r|S\rangle$ is low because many of the avalanches have already ended. The plots collapse onto a scaling function $Bx \exp(-Cx^2/2)$ with $B = 1.5 \times 10^{-3}$, $C = 1.8 \times 10^{-3}$, and $x = t/S^{\sigma\nu z}$.

The power spectra of the order parameter is shown in Fig. 5. The scaling regime exhibits a power-law exponent that is in accord with those used for the other collapses, $-1/\sigma\nu z = -1.8$. This supports the choice of scaling exponents we've made and is an additional support for the avalanche definition defined above because the power spectra do not depend on the definition of avalanches. A collapse is shown in the inset of Fig. 5 for the three largest K values. The collapse depends not only on rescaling by $\omega^{1/\sigma\nu z}$, but also rescaling the x axis by $(K_C - K)^{-\nu z}$ with $\nu z = 0.68$. This scaling form is given in Table I.

IV. DISCUSSION

By introducing a symmetry into the Kuramoto model in order to make the order parameter real, we are able to define and study avalanches in it, making it more analogous to other critical systems. The statistics of these avalanches reveal critical exponents and scaling functions which open up a new perspective on synchronizing phase transitions.

The analysis we have carried out is similar to analyses that have been done on different physical systems, such as slip avalanches in bulk metallic glasses and magnetization avalanches in Ising ferromagnets [2,3,5].

The analogy to depinning transitions drawn here is mostly qualitative rather than quantitative. Note that while the dynamics of running oscillators with large intrinsic phase velocities are not much affected by the slow-moving ones, the slow ones experience the noise generated by the fast ones. As a result this problem appears more challenging than standard elastic depinning problems such as elastic charge density wave depinning where all phases have the same average velocity [23,24] or the depinning of magnetic domain walls [25]. The Kuramoto model may be more similar to plastic depinning of charge density waves [9,26], which has the same avalanche statistics as the nonequilibrium random field Ising model [21,27]. As we show here, many of the same questions can be answered about the statistical and dynamical properties of the avalanches for the Kuramoto model, just as was previously done for many of these other avalanche models.

The exponents and scaling functions are predicted to be universal, depending only on general properties of the model such as symmetries and dimensions. They can be used to identify which experimental systems fall in the same universality class of systems with these same universal identifiers as the Kuramoto model. They can also be used to predict how big fluctuations can get in these synchronizing systems, which can be important for applications. Finally they bring another perspective to the field of avalanches because, contrary to most other systems with avalanches, no external driving force is involved in the Kuramoto system studied here. Rather the avalanches are triggered by the system's own internal dynamics.

We should note, however, that while the study here was performed at zero applied force or field, it is possible to extend the study to situations with an applied field [10]. In that case the system has two experimental tuning parameters: the coupling strength and the driving force. It will be interesting to explore that case in future studies, in order to develop a more general theory for how synchronizing systems fit into the larger context of avalanching systems.

APPENDIX: EXPONENTS INDEPENDENT OF SYSTEM SIZE

The simulations discussed in the body of the article were run with $N = 10^6$ oscillators. Identical simulations were run for a smaller system size of $N = 10^4$ oscillators. The

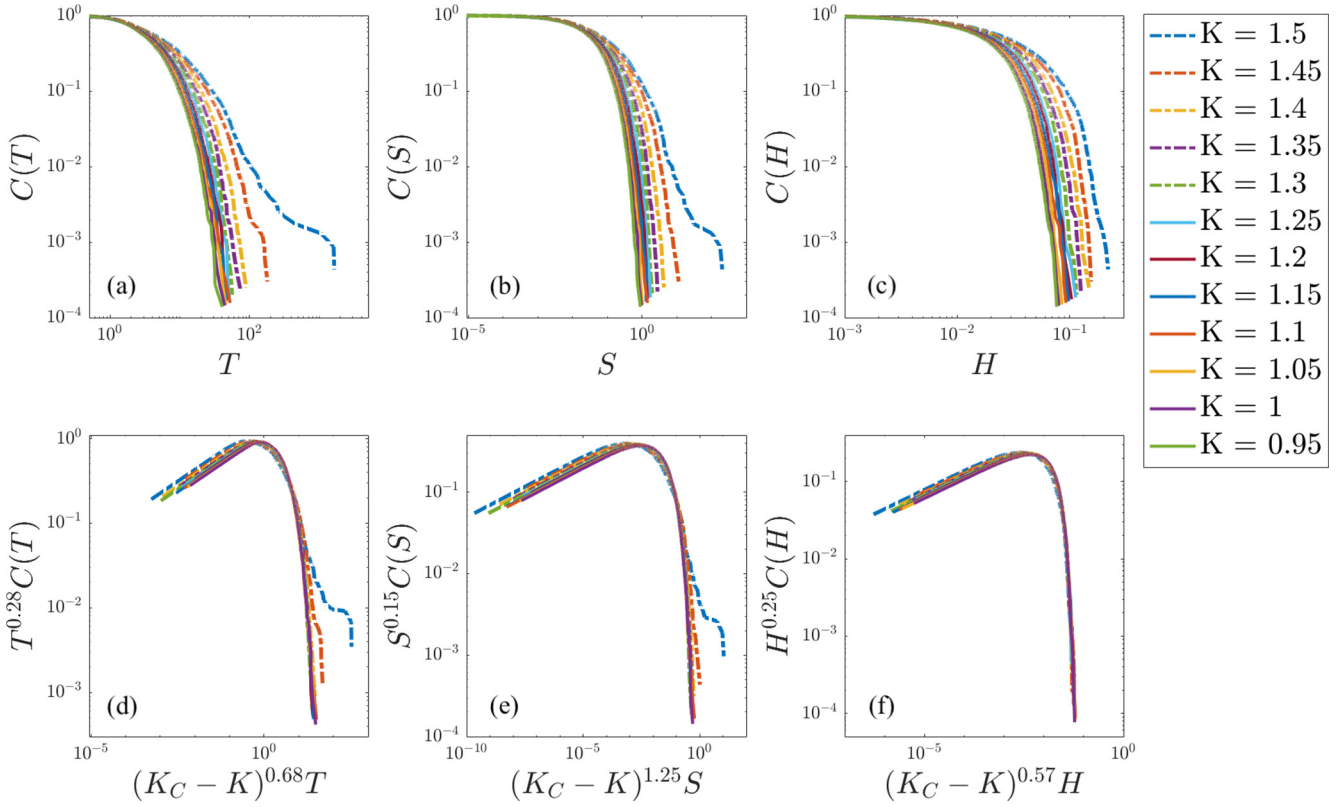

FIG. 6. (a)–(c) Complementary cumulative distribution functions (CCDFs) of the avalanche durations, T, sizes, S, and heights, H, for 12 values of the coupling strength K. The number of oscillators simulated here is $N = 10^4$. (d)–(f) Corresponding collapses of the CCDFs obtained by rescaling the x and y axes. The critical coupling value is $K_C \approx 1.596$. The values of the scaling exponents in the collapse are identical to the values used to collapse the CCDFs for the larger system size of $N = 10^6$. The CCDFs closest to the critical coupling strength show finite-size effects, as expected for the smaller system size.

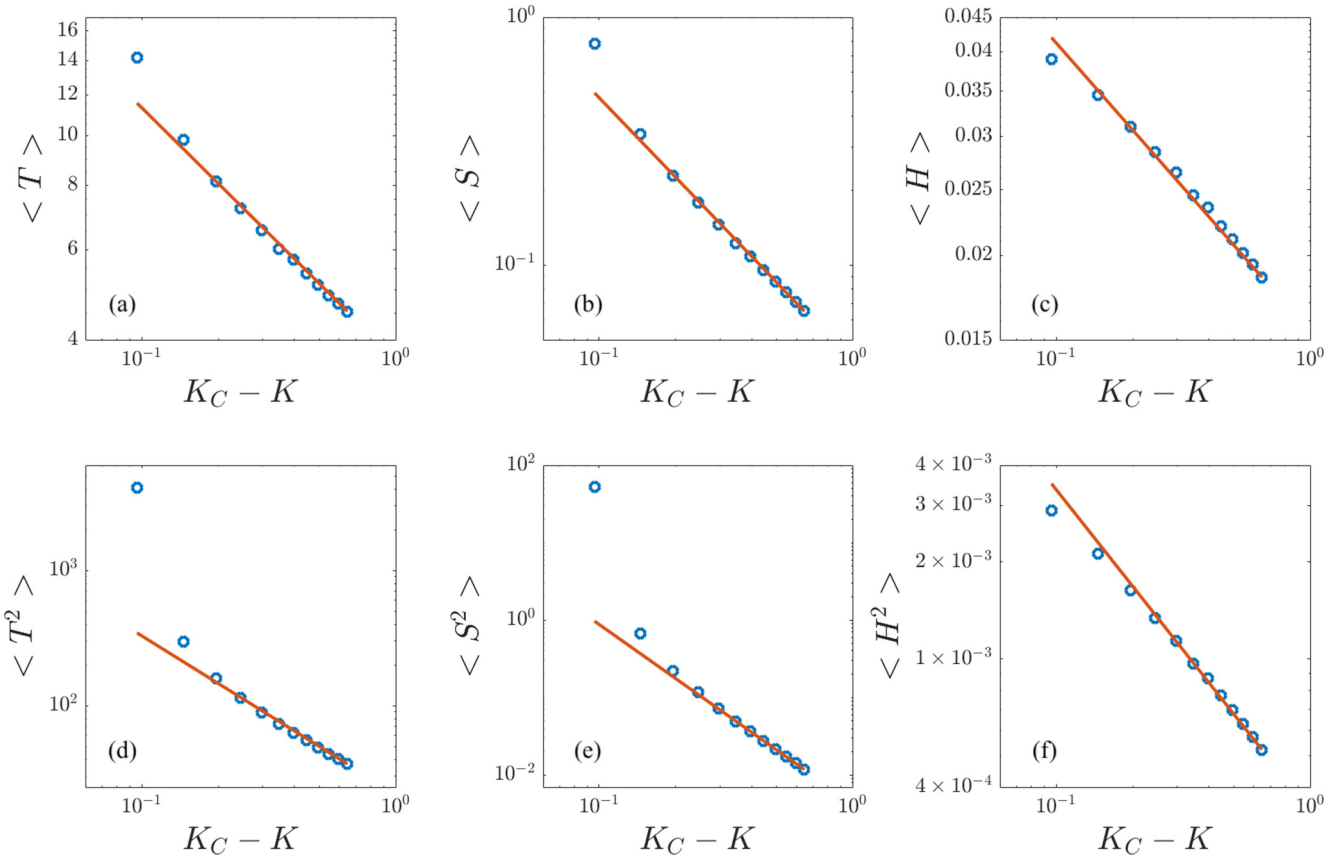

FIG. 7. (a)–(c) Average duration, T, size, S, and height, H, of avalanches for each value of the coupling constant from simulations with a system size of $N = 10^4$. The power-law scaling exponents are the same as those found for the larger system size of $N = 10^6$. The slopes for (a)–(c) are $-\nu z(-\alpha + 2) = -0.49$, $-1/\sigma(-\tau + 2) = -1.06$, and $-\rho(-\mu + 2) = -0.43$ respectively. (d)–(f) The average square duration, T, size, S, and height, H, of avalanches for each value of the coupling constant from simulations with a system size of $N = 10^4$. The slopes for (d)–(f) are $-\nu z(-\alpha + 3) = -1.2$, $-1/\sigma(-\tau + 3) = -2.3$, and $-\rho(-\mu + 3) = -1.0$, respectively. The power-law relationships, as well as the values of the scaling exponents, are given in Table I. Finite-size effects are visible close to the critical coupling strength, as expected for the smaller system size.

simulations were run for 12 values of the coupling constant: $K = 0.95, 1.00, 1.05, \ldots, 1.50$. For each value of the coupling constant, 20 random realizations were simulated drawing the natural speeds of the oscillators from a Gaussian distribution centered on zero with unit variance. Each realization was simulated for 2^{13} time steps with a step size of 0.2 s.

Figures 6 and 7 show the CCDFs and the average values of the same three metrics that are given in Figs. 2 and 3. The scaling exponents extracted from the larger-system-size simulations were used to collapse the CCDFs in Fig. 6. The same exponents are shown to describe the power-law scaling observed in Fig. 7. For the two coupling constant values closest to criticality, $K = 1.45$ and 1.50, finite-size effects are clearly visible. This is expected given the smaller system size and is why a much larger system size was chosen for the simulations in the body of the article.

[1] N. Goldenfeld, *Lectures on Phase Transitions and the Renormalization Group* (Addison-Wesley, Advanced Book Program, Redwood City, CA, 1992), Vol. 85.

[2] J. P. Sethna, K. A. Dahmen, and C. R. Myers, Nature (London) **410**, 242 (2001).

[3] J. Antonaglia, W. J. Wright, X. Gu, R. R. Byer, T. C. Hufnagel, M. LeBlanc, J. T. Uhl, and K. A. Dahmen, Phys. Rev. Lett. **112**, 155501 (2014).

[4] J. P. Coleman, F. Meng, K. Tsuchiya, J. Beadsworth, M. LeBlanc, P. K. Liaw, J. T. Uhl, R. L. Weaver, and K. A. Dahmen, Phys. Rev. B **96**, 134117 (2017).

[5] O. Perković, K. Dahmen, and J. P. Sethna, Phys. Rev. Lett. **75**, 4528 (1995).

[6] A. P. Mehta, A. C. Mills, K. A. Dahmen, and J. P. Sethna, Phys. Rev. E **65**, 046139 (2002).

[7] A. P. Mehta, K. A. Dahmen, and Y. Ben-Zion, Phys. Rev. E **73**, 056104 (2006).

[8] M. A. Sheikh, R. L. Weaver, and K. A. Dahmen, Phys. Rev. Lett. **117**, 261101 (2016).

[9] M. C. Marchetti and K. A. Dahmen, Phys. Rev. B **66**, 214201 (2002).

[10] J. A. Acebrón, L. L. Bonilla, C. J. P. Vicente, F. Ritort, and R. Spigler, Rev. Mod. Phys. **77**, 137 (2005).

[11] S. H. Strogatz, Physica D **143**, 1 (2000).

[12] C. Choi, M. Ha, and B. Kahng, Phys. Rev. E **88**, 032126 (2013).

[13] H. Daido, J. Stat. Phys. **60**, 753 (1990).

[14] H. Hong, H. Chaté, H. Park, and L.-H. Tang, Phys. Rev. Lett. **99**, 184101 (2007).
[15] H. Hong, H. Chaté, L.-H. Tang, and H. Park, Phys. Rev. E **92**, 022122 (2015).
[16] D. Mertens and R. Weaver, Phys. Rev. E **83**, 046221 (2011).
[17] D. Mertens and R. Weaver, Complexity **16**, 45 (2011).
[18] R. L. Weaver, O. I. Lobkis, and A. Yamilov, J. Acoust. Soc. Am. **122**, 3409 (2007).
[19] A. Yamilov, R. L. Weaver, and O. I. Lobkis, Photon. Spectra **2006**, 90 (2006).
[20] M. G. Kitzbichler, M. L. Smith, S. R. Christensen, and E. Bullmore, PLoS Comput. Biol. **5**, e1000314 (2009).
[21] J. P. Sethna, K. Dahmen, S. Kartha, J. A. Krumhansl, B. W. Roberts, and J. D. Shore, Phys. Rev. Lett. **70**, 3347 (1993).
[22] M. LeBlanc, L. Angheluta, K. Dahmen, and N. Goldenfeld, Phys. Rev. E **87**, 022126 (2013).
[23] O. Narayan and D. S. Fisher, Phys. Rev. B **46**, 11520 (1992).
[24] C. R. Myers and J. P. Sethna, Phys. Rev. B **47**, 11171 (1993).
[25] H. Ji and M. O. Robbins, Phys. Rev. B **46**, 14519 (1992).
[26] M. C. Marchetti, A. A. Middleton, and T. Prellberg, Phys. Rev. Lett. **85**, 1104 (2000).
[27] K. Dahmen and J. P. Sethna, Phys. Rev. B **53**, 14872 (1996).